JACC: CARDIOVASCULAR IMAGING VOL. 2, NO. 2, 2009

ISSN 1936-878X/09/$36.00
PUBLISHED BY ELSEVIER INC. DOI:10.1016/j.jcmg.2008.09.012

Changes in Myocardial Perfusion Correlate With Deterioration of Left Ventricular Systolic Function in Chronic Chagas' Cardiomyopathy

Flávio C. Hiss, MD, Thiago F. Lascala, MD, Benedito C. Maciel, MD, PhD, José A. Marin-Neto, MD, PhD, FACC, Marcus V. Simões, MD, PhD

São Paulo, Brazil

OBJECTIVES This study aimed at analyzing the association between myocardial perfusion changes and the progression of left ventricular systolic dysfunction in patients with chronic Chagas' cardiomyopathy (CCC).

BACKGROUND Pathological and experimental studies have suggested that coronary microvascular derangement, and consequent myocardial perfusion disturbance, may cause myocardial damage in CCC.

METHODS Patients with CCC (n = 36, ages 57 ± 10 years, 17 males), previously having undergone myocardial perfusion single-positron emission computed tomography and 2-dimensional echocardiography, prospectively underwent a new evaluation after an interval of 5.6 ± 1.5 years. Stress and rest myocardial perfusion defects were quantified using polar maps and normal database comparison.

RESULTS Between the first and final evaluations, a significant reduction of left ventricular ejection fraction was observed (55 ± 11% and 50 ± 13%, respectively; p = 0.0001), as well as an increase in the area of the perfusion defect at rest (18.8 ± 14.1% and 26.5 ± 19.1%, respectively; p = 0.0075). The individual increase in the perfusion defect area at rest was significantly correlated with the reduction in left ventricular ejection fraction (R = 0.4211, p = 0.0105). Twenty patients with normal coronary arteries (56%) showed reversible perfusion defects involving 10.2 ± 9.7% of the left ventricle. A significant topographic correlation was found between reversible defects and the appearance of new rest perfusion defects at the final evaluation. Of the 47 segments presenting reversible perfusion defects in the initial study, 32 (68%) progressed to perfusion defects at rest, and of the 469 segments not showing reversibility in the initial study, only 41 (8.7%) had the same progression (p < 0.0001, Fisher exact test).

CONCLUSIONS In CCC patients, the progression of left ventricular systolic dysfunction was associated with both the presence of reversible perfusion defects and the increase in perfusion defects at rest. These results support the notion that myocardial perfusion disturbances participate in the pathogenesis of myocardial injury in CCC. (J Am Coll Cardiol Img 2009;2:164–72) © 2009 by the American College of Cardiology Foundation

From the Division of Cardiology, University Hospital, Medical School of Ribeirão Preto, University of São Paulo, Brazil. Dr. Simões is the recipient of a research grant from Conselho Nacional de Desenvolvimento Científico e Tecnológico (#307153/2004-5).

Manuscript received May 27, 2008; revised manuscript received August 29, 2008, accepted September 9, 2008.

Chronic Chagas' cardiomyopathy (CCC) is a serious public health problem on the Latin American subcontinent, representing one of the major causes of heart failure and sudden death in many regions (1). The slow progression of myocardial damage occurs over a prolonged period of 2 to 3 decades. During the more advanced phases of the disease, there is an intense dilation of all cardiac chambers and severe systolic dysfunction of both ventricles that associates with heart failure, malignant ventricular arrhythmia, and thromboembolic phenomena (2). Despite the high morbidity and mortality associated with CCC, its pathogenesis is still poorly understood (3).

See page 173

It is believed that myocardial damage is mainly dependent on parasitism of myocardial fibers by *Trypanosoma cruzi* and aggression of nonparasitized tissue by an autoimmune reaction. In addition, several lines of evidence, including autopsy studies in humans (4,5) and experimental investigations (6,7), suggest that derangements of the coronary microcirculation may impair regional myocardial perfusion, producing myocytolysis and reparative fibrosis (3).

In agreement with this hypothesis, several clinical studies using myocardial perfusion scintigraphy have demonstrated a high prevalence of reversible perfusion defects in patients with CCC in the presence of angiographically normal subepicardial coronary arteries, suggesting the presence of abnormalities in the regulation of myocardial blood flow at the coronary microvascular level (8,9).

In a recent study of patients with CCC, we demonstrated a positive correlation between the extent of perfusion defects and the severity of left ventricular (LV) systolic dysfunction. In that study, reversible perfusion defects were detected in a sizable proportion of patients with early stages of Chagas' disease and normal LV systolic function (10). These data support the hypothesis that changes in myocardial perfusion may precede the onset of ventricular dysfunction and may participate in the pathogenesis of Chagas' cardiomyopathy. However, no longitudinal study has been conducted thus far to test this hypothesis.

Therefore, the objective of the present study was to investigate the correlation of progressive changes in myocardial perfusion at rest and during stress with the impairment of regional and global LV systolic function in patients with CCC and angiographically normal subepicardial coronary arteries.

METHODS

Study population. The study was conducted on 36 subjects with Chagas' disease being followed up at the outpatient clinics of the Cardiology Division, University Hospital, Medical School of Ribeirão Preto. The only inclusion criteria were to have a positive epidemiology and serologic tests for *T. cruzi* infection, and to have undergone myocardial perfusion scintigraphy and a 2-dimensional echocardiogram (ECG) at least 2 years before enrollment in the study.

Exclusion criteria were pregnancy, unstable clinical condition, or presence of comorbidities that might be associated with microvascular disease, such as diabetes mellitus, hypertension, cardiac valvular disease, history of obstructive coronary artery disease, and other forms of cardiomyopathy.

After enrollment, all patients had a full clinical and laboratory evaluation including a standard 12-lead resting ECG, a resting transthoracic 2-dimensional ECG, and a new scintigraphic study of myocardial perfusion at rest and under stress. The results obtained during this late phase of evaluation were compared with those obtained at the initial evaluation. The mean interval between the 2 evaluations was 5.6 ± 1.5 years.

ABBREVIATIONS AND ACRONYMS

CCC = chronic Chagas' cardiomyopathy
ECG = electrocardiogram
LV = left ventricular
LVEF = left ventricular ejection fraction
SPECT = single-photon emission computed tomography

Twenty of the 36 patients showed reversible perfusion defects and underwent coronary angiography, which ruled out the presence of obstructive coronary artery disease of subepicardial vessels.

The study was conducted according to the precepts of the Helsinki Declaration and was approved by the Research Ethics Committee of our institution. All patients gave written informed consent to participate.

Myocardial perfusion scintigraphy. The scintigraphic studies were performed using a digital DST camera (Sopha Medical Vision, Twinsburg, Ohio) equipped with a double detector, a wide rectangular view field, a dedicated processor (NXT-P, Sopha Medical Vision), and low-energy and high-resolution collimators.

The single-positron emission computed tomography (SPECT) images were acquired with the patient in the supine position, with a semicircular

orbit (from the right anterior oblique projection to the left posterior oblique projection), at 180°, in 32 projections, 60 s/projection. Symmetric 20% energy windows centered on the energy peak were used for the 2 isotopes employed, namely, thallium-201 (70 keV) and technetium-99m (140 keV). Acquisition matrices of 64 × 64 pixels were used, with a pixel size of 0.6 cm. The tomographic images were corrected for field uniformity and center of rotation.

All anti-ischemic medications were discontinued for 48 h before the study. Exercise treadmill (n = 11) or vasodilating stimulation with dipyridamole (n = 25) was used as the stress test. Sestamibi-Tc99m and thallium-201 were used as radiotracers of regional myocardial blood flow. The imaging protocol with sestamibi-Tc99m included the injection of 12 to 15 mCi at rest and 25 to 30 mCi at the peak of stress 3 to 4 h later, with the images being acquired 60 min after injection of the radiopharmaceutical. The protocol for thallium-201 consisted of injections of 3 to 4 mCi at the peak of stress, with image acquisition within 10 min, followed by redistribution images 3 to 4 h afterward.

Processing and analysis of the scintigraphic images. Tomographic sections on the 3 orthogonal planes were calculated according to the axis of the heart. Polar maps were constructed by using commercially available software (MyoQuant Liege, Sopha Medical Vision). The left ventricular surface was divided into 17 segments for the analysis of myocardial perfusion and used for correlation with the visual analysis of segmental regional mobility in the echocardiographic study.

Quantitative analysis was carried out by comparing the polar maps of the patients with a data bank for normal persons under the same physiological conditions (rest/stress) and for sex and isotope used (technetium-99m or thallium-201). Myocardial regions showing uptake values below 2.5 SD in relation to the mean value for normal subjects were identified as uptake defects.

For each image obtained at rest or under stress, we calculated the total area of the perfusion defect and the index of the perfusion defect, defined as the product of the area by the mean intensity of the defect. A global reversibility index was calculated for each patient by subtracting the indexes obtained in the stress-rest images.

For analysis of the topographic correlation of changes in perfusion, and for serial myocardial perfusion imaging evaluation, the polar maps were visually assessed by 2 experienced observers and the discordances solved by consensus. The segments exhibiting an uptake defect on at least two-thirds of their surface were defined as having an uptake defect. The segments presenting an uptake defect in the images of the stress phase, but not in the images of the rest phase, were defined as having a reversible defect.

Echocardiographic study. The examinations were carried out by trained echocardiographers and stored as high-resolution VHS images. The initial and late examinations were analyzed off-line by a single experienced echocardiographer who was blinded regarding clinical and scintigraphic data, as well as to the phase of the study.

Images of sections on the long and short parasternal axes and apical 2- and 4-chamber views were obtained. Global systolic function of the left ventricle was evaluated by calculation of the ejection fraction (EF) in the apical 2- and 4-chamber sections by the method of Simpson. Segmental wall motion was analyzed by dividing the left ventricle into 17 segments. A semiquantitative visual mobility score was attributed to each segment: 1 = normal mobility, 2 = hypokinesis, 3 = akinesis, and 4 = dyskinesis. A segmental wall motion index for the left ventricle was calculated for each patient as the sum of the scores divided by the total number of segments evaluated.

Statistical analysis. Data are reported as mean ± SD. The Kolmogorov-Smirnov test was used to determine whether the variables showed normal distribution. For the comparison of the means and/or the determination of correlation between variables with non-normal distribution, we used the nonparametric Wilcoxon matched-pairs signed-ranks and Spearman rank correlation tests, respectively. For variables with normal distribution, we used the paired *t* test and the Pearson correlation test. Fisher's exact test was used to test the topographic association between LV regional function and perfusion changes. The level of significance was set at $p < 0.05$ in all analyses.

RESULTS

Table 1 presents the general demographic, clinical, and laboratory characteristics of the patients at the time of the first and final evaluations.

Evaluation of LV function. Left ventricle ejection fraction (LVEF) evaluated by 2-dimensional echocardiogram showed a significant reduction between the initial (55.0 ± 11.0%) and the late examination (50.0 ± 13%; p = 0.0001, Wilcoxon test). Analysis of segmental wall motion in the initial study re-

Table 1. Demographic, Clinical, and Laboratory Characteristics of the Patients (n = 36) at the Time of Initial and Late Myocardial Perfusion SPECT and Echocardiographic Evaluations

	Initial Evaluation	Late Evaluation
Sex, male	17 (47%)	17 (47%)
Age, yrs	57 ± 10	63 ± 10
Symptoms		
Dyspnea	16 (44%)	14 (39%)
Precordial pain	25 (69%)	9 (25%)*
Palpitations	12 (33%)	5 (14%)*
Dizziness	6 (17%)	5 (14%)
NYHA functional class		
I	27 (75%)	26 (72%)
II	6 (17%)	8 (22%)
III	2 (5%)	2 (5%)
IV	1 (3%)	0
Resting electrocardiogram		
Left anterior hemiblock	11 (31%)	13 (36%)
Right bundle branch block	14 (39%)	16 (44%)
Left bundle branch block	2 (5%)	2 (5%)
Ventricular ectopic beat	7 (19%)	4 (11%)
Atrial fibrillation	4 (11%)	4 (11%)
Pacemaker	7 (19%)	17 (47%)*
Inactive electric zone	2 (5%)	2 (6%)
Medications		
Acetylsalicylic acid	7 (19%)	11 (31%)
Amiodarone	8 (22%)	14 (39%)*
Calcium-channel antagonist	2 (5%)	0
Beta-blocker	6 (17%)	18 (50%)*
Digitalis	1 (3%)	5 (14%)
Diuretics	9 (25%)	14 (39%)*
ACE inhibitor	19 (53%)	26 (72%)*
Nitrates	2 (5%)	3 (8%)

*$p < 0.05$ for comparison with the initial evaluation (paired proportion test). ACE = angiotensin-converting enzyme; NYHA = New York Heart Association; SPECT = single-positron emission computed tomography.

vealed that 23 (64%) patients had dysynergy in at least 1 regional segment of the left ventricle. Of the 612 segments analyzed, 172 (28%) presented dysynergy, 128 hypokinetic, 31 akinetic, and 13 dyskinetic, with a mean of 4.8 abnormal segments per patient. The mean initial segmental wall motion index was 1.4 ± 0.39.

In the late analysis, 27 patients (75%) presented dysynergy in at least 1 LV regional segment. A total of 248 dysynergic segments were detected among the 612 segments analyzed (40.5%), with a mean of 6.9 abnormal segments per patient. Of these, 171 presented hypokinesis, 66 akinesis, and 11 dyskinesis. Thus, the mean index of segmental wall motion was 1.5 ± 0.48 in the late evaluation, corresponding to a significant increase compared to the initial evaluation ($p = 0.0003$, Wilcoxon test).

The topographic distribution of left ventricle segments showing dysynergy and perfusion abnormalities in the initial and late study is presented in Table 2. It can be seen that the appearance of new wall motion defects predominated in the apical region and in the inferior and inferolateral walls of the left ventricle.

Perfusion defects at rest. Uptake defects at rest were identified in 27 of the 36 (75%) patients in the initial study and in 28 of the 36 (77.8%) in the late study. Of the 612 segments analyzed, 98 (16%) presented perfusion defects at rest in the initial study, and 158 (25.8%) presented defects in the late study. The topographic distribution of the segments exhibiting a perfusion defect at rest is also shown in Table 2. A predominant involvement of the inferolateral, inferior, and apical walls of the left ventricle was observed.

A significant increase in the index of uptake defect (incorporating area and severity) at rest was observed between the initial study (5.5 ± 5.2%) and the late study (9.3 ± 8.3%; $p = 0.0013$, Wilcoxon test). The same behavior was detected when the areas of the defects at rest were compared between the initial study (18.8 ± 14.1%) and the late study (26.5 ± 19.1%; $p = 0.0075$, paired t test).

Table 2. Frequency Distribution of the Left Ventricular Segments Showing Wall Motion and Perfusion Disorders According to a 17-Segments Model

Segments	Alteration of Parietal Mobility		Initial Reversible Perfusion Defect	Perfusion Defect at Rest	
	Initial	Late		Initial	Late
Basal anteroseptal	5	6	0	0	1
Basal anterior	3	5	0	0	0
Basal anterolateral	11	11	2	1	5
Basal inferolateral	15	20	5	13	20
Basal inferior	22	21	5	7	17
Basal inferoseptal	12	13	0	0	4
Mid-anteroseptal	3	8	2	0	1
Mid-anterior	5	7	2	0	1
Mid-anterolateral	8	10	1	2	2
Mid-inferolateral	15	21	7	10	18
Mid-inferior	12	17	5	7	17
Mid-inferoseptal	5	12	2	1	1
Apical septal	9	19	3	5	7
Apical anterior	11	19	1	4	8
Apical lateral	12	18	3	12	13
Apical inferior	13	19	3	19	23
Apex	11	22	6	17	20
Total	172	248	47	98	158

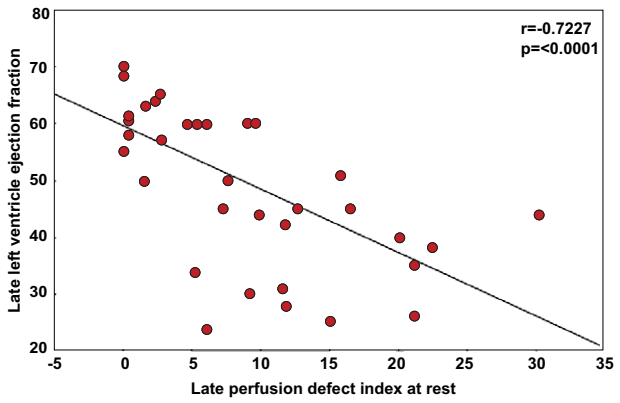

Figure 1. Correlation Between Rest Perfusion Defect and LV Systolic Function

This scatter plot demonstrates the significant negative correlation between the perfusion defect index (integrating extent and severity) obtained by using myocardial perfusion single-positron emission computed tomography imaging at rest and the correspondent individual value of the left ventricular (LV) ejection fraction assessed by bi-dimensional echocardiogram ($R = -0.7227$; $p < 0.0001$, Spearman correlation test). This result indicated that in patients with chronic Chagas' cardiomyopathy, the degree of LV systolic dysfunction correlates with the extent/severity of the perfusion defect at rest, which possibly corresponds to areas of regional myocardial fibrosis.

Reversible perfusion defects. In the initial scintigraphic study, reversible perfusion defects were detected in 20 (56%) patients, involving 47 of 612 segments (7.6%). The topographic distribution of the frequency of segmental involvement is summarized in Table 2.

Considering the subgroup of 20 patients who exhibited reversible perfusion defects in the initial study, a reduction of the reversibility index for the perfusion defects was observed between the initial study (3.4 ± 3.1%) and the late study (1.5 ± 2.4%; $p = 0.044$, Wilcoxon test). The same result was obtained when the reduction of the area of reversible defects was compared between the initial study (10.2 ± 9.7%) and the late study (3.19 ± 10.9%; $p = 0.012$, Wilcoxon test).

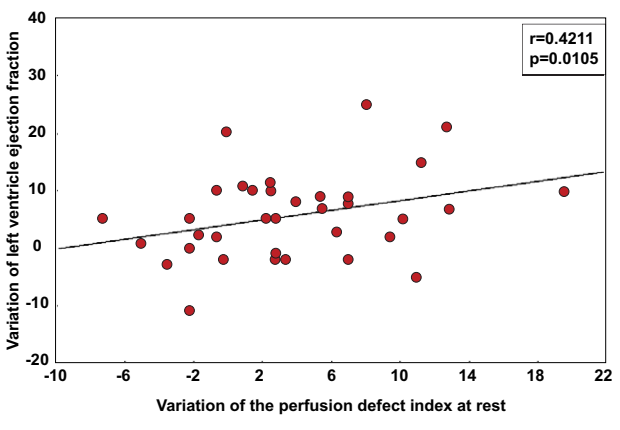

Figure 2. Correlation Between Changes of Rest Perfusion Defects and LV Function

This scatter plot illustrates the significant positive correlation between the increase in the index of perfusion defect at rest and the degree of left ventricular (LV) ejection fraction reduction observed between the initial and late evaluations ($R = 0.4211$; $p = 0.0105$, Pearson correlation test). This result indicates that the progression of global LV dysfunction correlates with the aggravation of the extent and severity of perfusion defects at rest, possibly signaling the increase in the areas of myocardial fibrosis.

Correlation between changes in myocardial perfusion and LV systolic function. A significant topographic association was observed between the presence of perfusion defects and segmental wall motion abnormalities at the late scintigraphic and echocardiographic studies. Of the 178 segments exhibiting perfusion defects, 128 (72%) presented changes in regional mobility, whereas of the 434 segments without perfusion defects, only 120 (28%) had wall motion abnormalities ($p < 0.0001$, Fisher exact test). Additionally, a significant negative correlation was observed between the index of perfusion defects at rest detected in the final scintigraphic study and the correspondent LVEF ($R = -0.7227$; $p < 0.0001$, Spearman correlation test) (Fig. 1).

Regarding the progression of perfusion and function changes, a significant positive correlation was observed between the increase in the index of perfusion defect at rest and the reduction of LVEF between the 2 evaluations ($R = 0.4211$; $p = 0.0105$, Pearson correlation test) (Fig. 2).

Association between reversible perfusion defects and progression of myocardial uptake defects at rest. A higher frequency of new perfusion defects at rest in the late study was seen in the segments exhibiting reversible defects in the initial study. Of the 47 segments presenting reversible perfusion defects in the initial study, 32 (68%) progressed to perfusion defects at rest, and of the 469 segments not showing reversibility in the initial study, only 41 had the same progression (8.7%; $p < 0.0001$, Fisher exact test). An illustrative example of a patient of this series, presenting reversible perfusion defects in the initial myocardial perfusion study topographically correlated to the region of rest perfusion defect in the final evaluation, is displayed in Figure 3.

Other correlations. No significant correlation was found between the initial stress or rest scores and the deterioration of LV function over time. Neither was any correlation found between perfusion defect scores and the tracer used. Finally, no differences were observed in the topographic distribution of perfusion defects regarding sex.

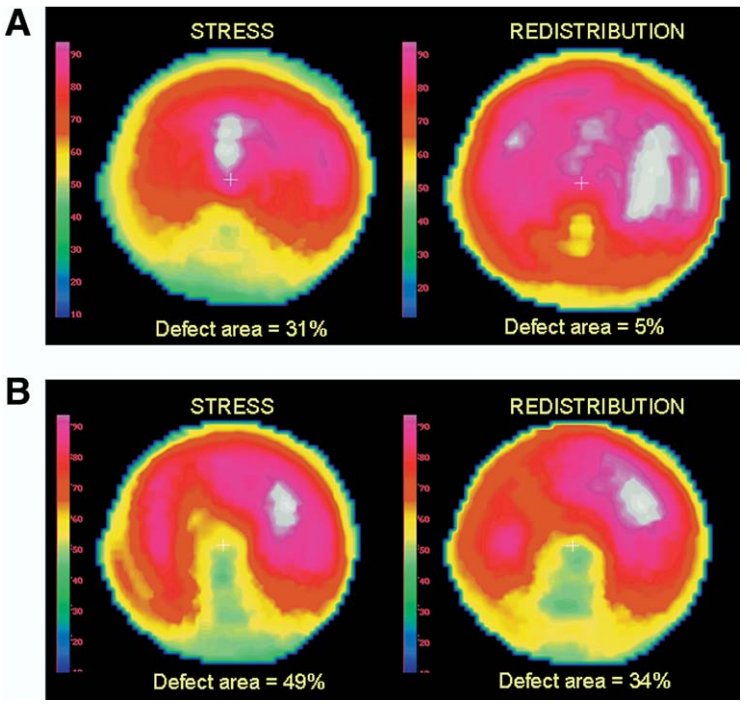

Figure 3. Stress and Redistribution Polar Maps of Initial and Late SPECT Thallium-201 Myocardial Perfusion Studies

Stress and redistribution polar maps of the initial **(A)** and late **(B)** single-positron emission computed tomography (SPECT) thallium-201 myocardial perfusion study of a patient enrolled in the study. The interval between images was 6.5 years. The left ventricular ejection fraction at the time of the initial study was 36% and declined to 31% at the late evaluation. A large, predominantly reversible myocardial perfusion defect involving the apex, septal, inferoseptal, inferior, and inferolateral walls is seen in the initial study. In the late study, an extensive rest perfusion defect is observed in the same topography.

DISCUSSION

Perfusion defects at rest and progression of systolic dysfunction. The correlation between perfusion defects at rest and myocardial fibrosis has been described in patients with dilated cardiomyopathy studied with endomyocardial biopsies or through autopsy investigations (11). Previous findings from our laboratory showed that chagasic patients with angiographically normal coronary arteries had fixed perfusion defects at planar thallium-201 stress-rest myocardium scintigraphy in left ventricle segments with severe dysynergy (akinesis or dyskinesis), possibly denoting the presence of cardiac fibrosis (9). In another observational cross-section study, we used SPECT thallium-201 scintigraphy for the evaluation of 37 patients in various stages of Chagas' heart disease and demonstrated perfusion defects (fixed, paradoxical, or reversible) in 78% of the patients. In this later investigation, the extent of the perfusion defects at rest correlated with the degree of LV systolic dysfunction (10). With the present study, we provide the first longitudinal observation in patients with CCC showing that the progression of both segmental and global LV dysfunction correlates with the aggravation of the extent and severity of perfusion defects at rest, possibly signaling the increase in the areas of myocardial fibrosis.

These results agree with pathology studies on human hearts showing that myocardial fibrosis is a most prominent histopathological feature of CCC that is correlated with the degree of impairment of cardiac function (12). Also, a recent study using magnetic resonance imaging showed in vivo evidence of more marked myocardial fibrosis in more advanced forms of chagasic cardiomyopathy (13).

Even though a significant association was found between the temporal reduction in LVEF and the concomitant increase of regional myocardial fibrosis, the correlation between these variables was not strong ($R = 0.42$) (Fig. 2). This probably reflects the effect of other determinants of progression of LV dysfunction, besides coalescence of regional fibrosis, such as active diffuse focal myocarditis (14).

Reversible perfusion defects. In the present study, the initial myocardial perfusion SPECT scans dem-

onstrated reversible perfusion defects in a large proportion of patients (55%) in the absence of angiographically significant obstructive epicardial coronary disease. This finding suggests that reversible myocardial ischemia in those patients is due to disorders at the level of the coronary microcirculation (15) and confirms previous studies of Chagas' heart disease that reported similar findings (8–10).

However, this is the first time that a topographic correlation was found between reversible perfusion defects and the later appearance of new perfusion defects at rest that correlated with deterioration of segmental and global systolic LV dysfunction. This observation strongly suggests a correlation between disorders in the coronary microcirculation and the progression of regional myocardial fibrosis, as previously postulated from experimental and human pathology evidence. Thus, autopsy studies have reported diffuse collapse of intramyocardial arterioles, with luminal constriction attributed to intimal proliferation (4). Notably, these microvascular abnormalities correlated topographically with the extension of diffuse myocytolysis and myocardial fibrosis. Also, studies of biopsy specimens showed extensive microvascular abnormalities, including thickening of the basal capillary membrane (16). Abnormal vasodilation and vasoconstriction patterns at the microcirculatory level have been implicated as causing myocardial damage in patients with Chagas' disease (17). Finally, studies in the experimental murine model of Chagas' disease have demonstrated microcirculatory disorders such as formation of occlusive platelet thrombi in the epicardiac and small intramural coronary arteries, leading to myocardial ischemia detectable by histochemical methods in vivo (6). The mechanisms responsible for the formation of occlusive platelet thrombi and microcirculatory spasm include injury to endothelial cells by *T. cruzi* infection (18), increased local production of endothelin and thromboxane-A2 by the infected tissue, and increased production of cytokines by the chronic inflammatory infiltrate, leading to abnormal microvascular reactivity (19).

It is worth emphasizing that microvascular coronary dysfunction is not a particular feature of Chagas' cardiomyopathy, as it has also been recognized in patients with ventricular dysfunction caused by dilated cardiomyopathy due to other causes (20,21). In an even more relevant manner, it has been demonstrated that the degree of microvascular coronary dysfunction is an independent predictor of cardiac events in patients with dilated cardiomyopathy, being associated with an increased risk of death and with additional progression of heart failure (22,23). The prognostic implications of coronary microvascular dysfunction for CCC await confirmation by a prospective study specifically designed to assess that hypothesis.

Pathophysiologic implications. It is plausible to assume that, similar to obstructive epicardial coronary artery disease, repeated ischemic phenomena in chronic Chagas' heart disease may cause myocytolytic necrosis with consequent coalescent cicatricial injuries related to the areas of regional transmural fibrosis identified during the more advanced phases of CCC.

We can also speculate that repeated ischemic events in chronic Chagas' heart disease may cause transient regional LV contractile dysfunction due to a phenomenon of myocardial stunning, with late development of persistent contractile dysfunction similar to hibernating myocardium (24). This mechanism can explain the observation of segmental wall motion impairment in left ventricle regions with ischemic viable myocardium in CCC patients and normal coronary arteries (10). This hypothesis is compatible with preliminary studies showing improved LV function in patients with Chagas' disease acutely treated with isosorbide dinitrate (25) and taking dipyridamole for prolonged periods of time (26). In those studies, however, no clear relation was demonstrated between improvement of LV function and relief of myocardial ischemia.

Finally, the elucidation of the mechanism mediating the regional LV wall motion and perfusion changes needs further studies, mainly correlating these findings with histopathological observations.

Study limitations. In the present study, the assessment of the LV myocardial perfusion and wall motion were performed by using 2 different imaging techniques. This may have caused some degree of topographic mismatch during the analysis. A simultaneous evaluation of LV perfusion and function by using gated SPECT imaging would have circumvented this problem.

Because both thallium-201 and sestamibi labeled with technetium-99m were used for the studies of myocardial perfusion in various patients, to correct for possible differences between these radiopharmaceuticals in the detection of perfusion abnormali-

ties, quantitative analyses based on polar maps and comparisons with normal data bases were made.

Even though obstructive coronary artery disease was excluded in the patients presenting reversible perfusion defects in the initial evaluation, we cannot exclude entirely that coronary artery disease may have developed in a patient during the follow-up period.

CONCLUSIONS

This is the first study to observe and correlate longitudinal changes of both myocardial perfusion and LV wall motion abnormalities in the same group of patients with CCC followed up for a significant period of time. On the basis of the results obtained, the increase in perfusion defects at rest was clearly correlated with the progression of LV systolic dysfunction. In addition, reversible perfusion defects detected at the initial evaluation were topographically correlated with the development of new perfusion defects at rest at the later study, indicating the installation of new areas of fibrosis, as the disease progresses in patients with angiographically normal coronary arteries. These results lend support to the notion that regional abnormalities of LV perfusion, possibly caused by microvascular derangements, participate in the pathogenesis of myocardial damage in CCC.

Reprint requests and correspondence: Dr. Marcus V. Simões, Divisão de Cardiologia, Hospital das Clínicas da Faculdade de Medicina de Ribeirão Preto, Ribeirão Preto, São Paulo 14048-900, Brazil. *E-mail: msimoes@fmrp.usp.br.*

REFERENCES

1. World Health Organization. Control of Chagas' disease: second report of the WHO Expert Committee. Technical report series 905. Geneva: World Health Organization, 2002.
2. Morris SA, Tanowitz HB, Wittner M, Bilezikian JP. Pathophysiological insights into the cardiomyopathy of Chagas' disease. Circulation 1990;82:1900–9.
3. Marin-Neto JA, Cunha-Neto E, Maciel BC, Simões MV. Pathogenesis of chronic Chagas heart disease. Circulation 2007;115:1109–123.
4. Torres CM. [Arteriosclerosis of the fine arterial branches of the myocardium (Chagas' coronaritis) and focal myocytolysis in chronic Chagas' heart disease.] O Hospital 1958;54:19–34.
5. Köberle F. Pathogenesis of Chagas' disease. Ciba Found Symp 1974;20:137–58.
6. Rossi MA, Gonçalves S, Ribeiro-dos-Santos R. Experimental *Trypanosoma cruzi* cardiomyopathy in BALB/c mice: the potential role of intravascular platelet aggregation in its genesis. Am J Pathol 1984;114:209–16.
7. Morris SA, Weiss LM, Factor S, Bilezikian JP, Tanowitz H, Wittner M. Verapamil ameliorates clinical, pathologic and biochemical manifestations of experimental chagasic cardiomyopathy in mice. J Am Coll Cardiol 1989;14:782–9.
8. Hagar JM, Rahimtoola SH. Chagas' heart disease in the United States. N Engl J Med 1991;325:163–8.
9. Marin-Neto JA, Marzullo P, Marcassa C, et al. Myocardial perfusion abnormalities in chronic Chagas' disease as detected by thallium-201 scintigraphy. Am J Cardiol 1992;69:780–4.
10. Simões MV, Pintya AO, Bomberg-Marin G, et al. Relation of regional sympathetic denervation and myocardial perfusion disturbance to wall motion impairment in Chagas' cardiomyopathy. Am J Cardiol 2000;86:975–81.
11. Li LX, Nohara R, Okuda K, et al. Comparative study of 201Tl-scintigraphic image and myocardial pathologic findings in patients with dilated cardiomyopathy. Ann Nucl Med 1996;10:307–14.
12. Rossi MA. Patterns of myocardial fibrosis in idiopathic cardiomyopathies and chronic chagasic cardiopathy. Can J Cardiol 1991;7:287–94.
13. Rochitte CE, Oliveira PF, Andrade JM, et al. Myocardial delayed enhancement by magnetic resonance imaging in patients with Chagas' disease: a marker of disease severity. J Am Coll Cardiol 2005;46:1553–8.
14. Higuchi ML, De Morais CF, Pereira Barreto, et al. The role of active myocarditis in the development of heart failure in chronic Chagas' disease: a study based on endomyocardial biopsies. Clin Cardiol 1987;10:665–70.
15. Camici PG, Crea F. Coronary microvascular dysfunction. N Engl J Med 2007;356:830–40.
16. Ferrans CS, Milei J, Tomiata Y, Storino RA. Basement membrane thickening in cardiac myocytes and capillaries in chronic Chagas' disease. Am J Cardiol 1988;61:1137–40.
17. Higuchi ML, Fukasawa S, De Bellotti G, Brito T, Parzianello LC, Ramires JA. Different microcirculatory and interstitial matrix patterns in idiopathic dilated cardiomyopathy and Chagas' disease: a three dimensional confocal microscopy study. Heart 1999;82:279–85.
18. Libby P, Alroy J, Pereira MEA. A neuraminidase from *Trypanosoma cruzi* removes sialic acid from the surface of mammalian myocardial and endothelial cells. J Clin Invest 1986;77:127–35.
19. Tanowitz HB, Burns ER, Sinha KA, et al. Enhanced platelet adherence and aggregation in Chagas' heart disease: a potential pathogenic mechanism for cardiomyopathy. Am J Trop Med Hyg 1990;43:274–81.
20. Neglia D, Parodi O, Gallopin M, et al. Myocardial blood flow response to pacing tachycardia and to dipyridamole infusion in patients with dilated cardiomyopathy without overt heart failure. A quantitative assessment by positron emission tomography. Circulation 1995;92:796–804.
21. Canetti M, Akhter M, Lerman A, et al. Evaluation of myocardial blood flow reserve in patients with chronic congestive heart failure due to idiopathic dilated cardiomyopathy. Am J Cardiol 2003;92:1246–9.
22. Rigo F, Gherardi S, Galderisi M, et al. The prognostic impact of coronary flow-reserve assessed by Doppler echocardiography in non-ischemic dilated cardiomyopathy. Eur Heart J 2006;27:1319–23.
23. Neglia D, Michelassi C, Trivieri MG, et al. Prognostic role of myocardial blood flow impairment in idiopathic left ventricular dysfunction. Circulation 2002;105:186–93.

JACC: CARDIOVASCULAR IMAGING, VOL. 2, NO. 2, 2009
FEBRUARY 2009:164–72

24. Camici PG, Wijns W, Borgers M, et al. Pathophysiological mechanisms of chronic reversible left ventricular dysfunction due to coronary artery disease (hibernating myocardium). Circulation 1997;96:3205–14.
25. Marin-Neto JA, Souza ACS, Maciel BC, Gallo L Jr., Iazigi N. [Radionuclide angiocardiographic evaluation of the effect of isosorbide dinitrate in patients with Chagas' disease]. Arq Bras Cardiol 1988;51:367–71.
26. Kuschnir E, Sgammini H, Castro R, Evequoz C, Ledesma R. [Chronic Chagas' cardiomyopathy: effects of dipyridamole on ventricular dynamics]. Arq Bras Cardiol 1983;41: 373–8.

Key Words: myocardial perfusion scintigraphy ■ chronic Chagas' cardiomyopathy ■ left ventricular function ■ microcirculation.